Atmospheric forcing on the drift of Arctic sea ice in 1989–2009

Timo Vihma,[1] Priit Tisler,[1] and Petteri Uotila[2]

Received 23 October 2011; revised 7 December 2011; accepted 15 December 2011; published 18 January 2012.

[1] Inter-annual variations in Arctic sea ice drift speed (V_i) in 1989–2009 were analyzed on the basis of buoy data and atmospheric circulation indices. In the circumpolar and eastern Arctic and the Fram Strait, the annual mean V_i was best explained by the sea level pressure (SLP) difference across the Arctic Ocean along meridians 270°E and 90°E, called as the Central Arctic Index (CAI). In general, V_i was more strongly related to CAI than to the Dipole Anomaly (DA). This was because CAI is calculated across the Transpolar Drift Stream (TDS), whereas the pressure patterns affecting DA sometimes move far from TDS. CAI also has the benefit of being a simple index, insensitive to the calculation method applied, whereas DA, as the second mode of a principal component analysis, is sensitive both to the time period and area of calculations. In summer, the circulation index most important for the circumpolar mean V_i was the SLP gradient across the Fram Strait. In the Canadian Basin in winter, the Arctic Oscillation index was most important. Circulation indices explained 48% of the variance of the annual mean V_i in the circumpolar Arctic, 38% in the eastern Arctic, and 25% in the Canadian Basin. The local air-ice momentum flux (τ) was always better than the 10 m wind speed in explaining V_i, but τ outperformed the circulation indices only in the Fram Strait. Atmospheric forcing did not explain the increasing trend in V_i in the period 1989–2009.
Citation: Vihma, T., P. Tisler, and P. Uotila (2012), Atmospheric forcing on the drift of Arctic sea ice in 1989–2009, *Geophys. Res. Lett.*, *39*, L02501, doi:10.1029/2011GL050118.

1. Introduction

[2] Atmospheric forcing on Arctic sea ice drift is closely connected to the sea ice extent in September [*Rigor and Wallace*, 2004]. According to *Ogi et al.* [2010], the combined effect of winter and summer wind forcing accounts for 50% of the variance of the change in September sea ice extent from one year to the next. The drift speed of Arctic sea ice has substantially increased since 1950s [*Hakkinen et al.*, 2008]. Looking at a longer time scale, the drift of the French schooner Tara from the Laptev Sea to the Fram Strait took only 15 months in 2006–2007 [*Gascard et al.*, 2008] compared to three years by Nansen's Fram for roughly the same route in 1894–1896. According to *Rampal et al.* [2009], the increase in drift speed since 1979 is related to thinner sea ice with reduced mechanical strength, whereas *Hakkinen et al.* [2008] concluded that the increase since 1950s is due to stronger winds, and *Spreen et al.* [2011] recognized the importance of both effects in 1992–2009 with the ice thinning likely more important. In addition, the wind direction strongly affects the drift speed. For example, Tara's fast drift was favored by prevailing winds aligned on the Transpolar Drift Stream (TDS) [*Ogi et al.*, 2008; *Vihma et al.*, 2008] - the direction of drift least restricted by coastal boundaries. In addition to the increasing trend, sea ice drift speed in the Arctic exhibits a large inter-annual variability [*Kwok*, 2009], which cannot be explained by ice thickness.

[3] The atmospheric factor directly driving local sea ice drift is the local air-ice momentum flux (τ), but indirectly and on a larger scale, Arctic sea ice drift is related to circulation indices such as the Arctic Oscillation (AO), North Atlantic Oscillation (NAO), and Pacific Decadal Oscillation (PDO); AO is the leading mode of principal component analysis of the circumpolar sea-level pressure (SLP), whereas PDO is that for the North Pacific sea surface temperature, and NAO characterizes the SLP difference between the Icelandic low and the Azores high. The recent dramatic sea ice changes suggest a decreasing control of AO and NAO on the Arctic sea ice cover [*Zhang et al.*, 2008]. *Maslanik et al.* [2007] concluded that the AO index is not a reliable indicator of the ice transport patterns that have favored reduced ice cover in the western and central Arctic since the late 1980s. According to *Wu et al.* [2006] and *Wang et al.* [2009] the Dipole Anomaly (DA; the second-leading mode of SLP anomaly in the Arctic) may better explain the sea ice variability.

[4] In this paper we analyze the atmospheric forcing on the drift of Arctic sea ice in 1989–2009 applying information on several circulation indices, supported by reanalysis results for the air-ice momentum flux and 10-m wind speed. Our objectives are (1) to find out which indices are most strongly related to inter-annual variations in sea ice drift speed, (2) to quantify these relationships, and (3) to interpret the physical mechanisms behind them. The importance of DA has recently received a lot of attention but we explain why a simple pressure difference across TDS controls the drift speed variability better than DA. We address the annual and seasonal mean drift speed in the circumpolar Arctic and separately in three sub-regions with different sea ice conditions: the Canadian Basin, Eastern Arctic, and the Fram Strait (Figure 1).

2. Data Sets and Methods

[5] We applied monthly values (based on data with 6–24 h resolution) of AO, NAO, DA, PDO, as well as the SLP gradient across the Fram Strait (PGF, as calculated by *Tsukernik et al.* [2010]). The data sets of NAO and AO, based on daily values, were obtained from the National Oceanic and Atmospheric Administration's (NOAA) Climate Prediction Centre (CPC), http://www.cpc.ncep.noaa.

[1]Finnish Meteorological Institute, Helsinki, Finland.
[2]CSIRO Marine and Atmospheric Research, Aspendale, Victoria, Australia.

0094-8276/12/2011GL050118

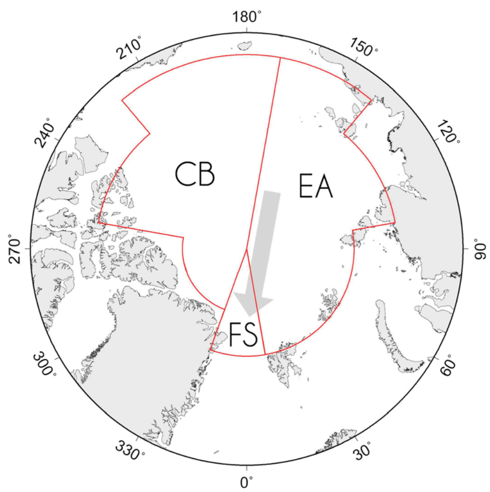

Figure 1. The area covered by the IABP data, with the subregions Canadian Basin (CB), Eastern Arctic (EA), and Fram Strait (FS). The gray arrow represents the Transpolar Drift Stream.

gov, and the PDO data from the University of Washington, http://jisao.washington.edu/pdo/. We calculated DA on the basis of 6-hourly data from (1) the ERA-Interim reanalysis of the European Centre of Medium-Range Weather Forecasts (ECMWF) and (2) the National Center for Environmental Prediction / Department of Energy (NCEP/DOE) reanalysis. With both data sources we used two approaches: the principal component analysis was (1) made separately for each season, as in the work of *Wang et al.* [2009], and (2) for the whole year. We accordingly got four sets of DA data, identified as $DA_{S,M}$ and $DA_{A,M}$, where subscripts S and A refer to the seasonal and annual principal component analyses, respectively, and M = ERA or NCEP. In addition, we defined a new Central Arctic Index (CAI) simply as the SLP difference between 270°E, x°N and 90°E, x°N, where x = 80, 82, or 84, yielding three sets of indices: CAI_{80}, CAI_{82}, and CAI_{84}, respectively. These were calculated on the basis of the 6-hourly ERA-Interim data. We also applied 6-hourly ERA-Interim data of the air-ice momentum flux (τ) and 10-m wind speed (V_{10}). For all variables, using the high-resolution (6-hourly or daily) values, we calculated the annual means and seasonal means for winter (DJF), spring (MAM), summer (JJA), and autumn (SON).

[6] The V_i data used in this study were based on a network of drifting automatic buoys, maintained by the International Arctic Buoy Programme (IABP). The data for 1979–2009 are available at the University of Washington from the internet host http://iabp.apl.washington.edu. However, we restricted the analysis to the period of 1989–2009 because (1) until 1985 the IABP buoy location data were only archived with 24 h time intervals, which reduces the calculated V_i due to the meandering drift [*Vihma and Launiainen*, 1993], (2) early IABP data were less accurate due to buoy positioning based on the Argos system instead of GPS, and (3) when this study was started, only the period since 1989 was covered by ERA-Interim. We use 12-hourly interpolated V_i estimates at fixed grid cells and focus on the scalar drift speed, but also present supporting analyses on the drift direction. Each grid cell south (north) of 80°N represents an area of 4° latitude × 20° (40°) longitude. For details of the data archive and processing, see *Rigor* [2002]. The total area covered by the buoy data is shown in Figure 1.

[7] In Section 3 we compare the seasonal and annual circulation indices against seasonal and annual ice drift speeds. As the original data sets had a temporal resolution of 6 to 24 h, the seasonal values include effects of high-frequency variability. We carry stepwise multiple regression analyses [*Draper and Smith*, 1998] to find out the large-scale factors that have the strongest statistical relationships with V_i. Only physically relevant relationships are included in the multiple regression equations.

3. Results

[8] In Figure 2 we show time series of those indices that reached statistically significant correlations with V_i. Note that the four results for DA include large differences (Figure 2c): although $DA_{A,ERA}$ and $DA_{A,NCEP}$ are practically identical (correlation coefficient r = 0.99), the seasonal values differ more (r = 0.69 between $DA_{S,ERA}$ and $DA_{S,NCEP}$), and the seasonal and annual values have a very low mutual correlation ($r < 0.2$). The three versions of CAI closely follow each other (Figure 2d; $r \geq 0.90$).

[9] The results of multiple regression analyses for the large-scale factors controlling V_i are shown in Table 1. Considering the annual mean in the Circumpolar Arctic, 48% of the inter-annual variance in V_i is statistically explained by a combination of CAI_{84} and $DA_{A,ERA}$. An even higher r^2 is reached for summer in the Circumpolar and Eastern Arctic and the Fram Strait, with PGF and CAI_{84} as the dominating explaining variables. For the annual mean and summer, statistically significant regression equations are found for all regions, and all r^2 values exceeding 0.4 occur in these periods. A significant regression equation for winter V_i is only found for the Canadian Basin, where AO alone is related to V_i. In autumn the only significant relationship occurs in the Fram Strait, with CAI_{82} explaining V_i. In Table 1, CAI (in some form) is the dominant variable in seven equations, PGF in three, and DA and AO both in one.

[10] We interpret the results by comparing the SLP fields and circulation indices. The physical background is that in free-drift conditions the ice motion is approximately parallel to SLP isobars [*Zubov*, 1943; *Thorndike and Colony*, 1982]; due to surface friction, the air-ice momentum flux deviates to the left of the geostrophic wind vector, but this is approximately balanced by the deviation of ice drift to the right of the air-ice momentum flux, which is due to the Coriolis force. We first checked how well this rule holds for the IABP data: as a circumpolar average over the 21 year period, in summer V_i deviated 8° to the left of the geostrophic wind, whereas in winter the deviation was 4° to the right. The results are relevant; ice is thinner in summer, and therefore the effect of the Coriolis force is not large enough to compensate the frictionally generated deviation. Hence, in the following we interpret that ice tends to drift in the direction of the geostrophic wind, but this may be prevented by coastal or internal resistance of a compact ice field.

[11] To compare the effects of CAI and DA on the ice drift, we calculated the SLP field averaged over the years with (1) four highest annual CAI values and (2) four lowest annual CAI values. Analogous calculations were made for DA (the years with the highest index values were different for CAI and DA, and only 2004 was common among the

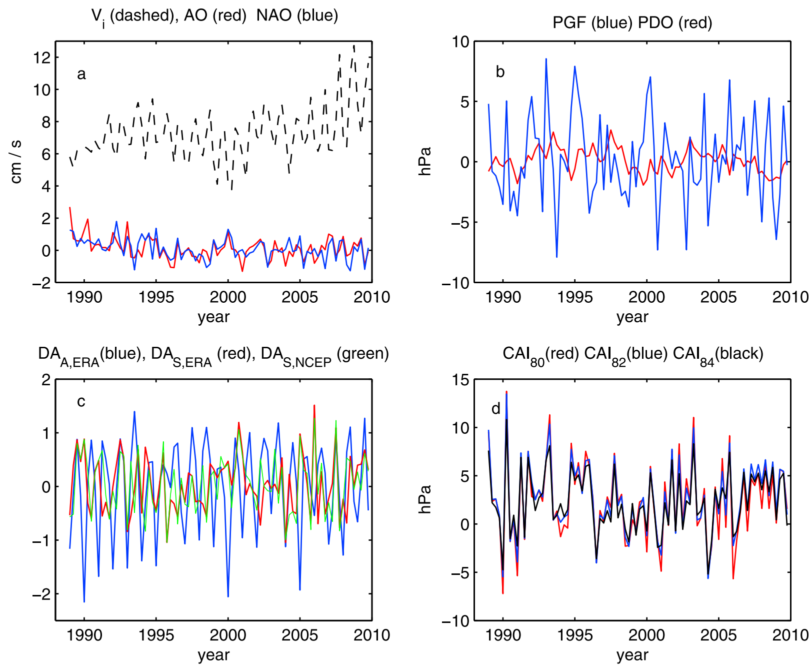

Figure 2. Time series of the seasonal means of (a) V_i (in cm/s) and AO and NAO (dimensionless); (b) PGF (in hPa) and PDO (dimensionless); (c) $DA_{A,ERA}$, $DA_{S,ERA}$, and $DA_{S,NCEP}$; and (d) CAI_{80}, CAI_{82}, and CAI_{84}. For clarity, $DA_{A,NCEP}$ is not shown as it closely matches $DA_{A,ERA}$.

years with the lowest values). In Figure 3 we show these results for CAI_{82} and $DA_{S,NCEP}$ (the results for the other forms of CAI and DA were qualitatively similar). Figure 3a reveals that the SLP isobars in years with a high CAI_{82} are almost perpendicular to those in years with a low CAI_{82}, whereas the angle between the isobars is smaller comparing years with a high and a low $DA_{S,NCEP}$ (Figure 3b). In years with a high CAI_{82} a strong geostrophic wind tends to drive ice motion along TDS, whereas in years with a low CAI_{82} a weaker geostrophic wind tends to drive ice motion from the Central Arctic towards the Canadian Arctic, where the ice does not have much freedom to drift.

[12] An example of the pressure field in SON 1998 further illustrates the better capability of CAI than DA in explaining V_i (Figure 4). $DA_{S,NCEP}$ was 0.18, exceeding its mean value of −0.06 by half a standard deviation, but CAI_{82} reached its lowest value (−2.3 hPa) during the whole period of 1989–2009. V_i in the Fram Strait reached its third lowest value (0.07 m/s), in accordance with a low CAI_{82}. The mean SLP field shows a pattern that clearly did not support a large V_i, but DA was larger than average due to the low in the Norwegian Sea and the high in the Central Arctic. Accordingly, the higher importance of CAI over DA (Table 1) originates from the fact that CAI is calculated across TDS, whereas the pressure patterns affecting DA sometimes move to locations less essential from the point of view of ice drift.

[13] Also PGF is calculated across a fixed line perpendicular to the prevailing ice drift, and PGF indeed reaches a high degree of explanation for V_i in JJA (Table 1). In all three sub-regions, a high summer PGF is associated with

Table 1. Multiple Regression Equations for V_i Calculated On the Basis of AO, NAO, PDO, DA_S, DA_A, and CAI for Latitudes 80°N, 82°N, and 84°N[a]

Region	Period	Multiple Regression Equation	r^2	BL-r^2	τ- r^2
Circumpolar Arctic	Annual	$V_i = 0.00365 \times CAI_{84} + 0.0226 \times DA_{A,ERA} + 0.06$	0.48	CAI_{84}: 0.27	0.23
Circumpolar Arctic	MAM	$V_i = 0.00115 \times CAI_{82} + 0.053$	0.29		0.27
Circumpolar Arctic	JJA	$V_i = 0.00305$ PGF $+ 0.0184\ DA_{A,NCEP} + 0.06$	0.54	PGF: 0.34	
Canadian Basin	Annual	$V_i = 0.0268 \times DA_{A,ERA} + 0.07$	0.25		
Canadian Basin	DJF	$V_i = -0.00678 \times$ AO $+ 0.06$	0.38		
Canadian Basin	JJA	$V_i = 0.00238 \times$ PGF $+ 0.07$	0.26		
Eastern Arctic	Annual	$V_i = 0.00455 \times CAI_{82} + 0.06$	0.38		0.32
Eastern Arctic	MAM	$V_i = 0.00164 \times CAI_{82} + 0.05$	0.37		0.38
Eastern Arctic	JJA	$V_i = 0.00308 \times$ PGF $+ 0.0245 \times DA_{A,ERA} + 0.06$	0.59	PGF: 0.35	0.23
Fram Strait	Annual	$V_i = 0.00543 \times CAI_{82} + 0.07$	0.24		0.36
Fram Strait	JJA	$V_i = 0.00431\ CAI_{84} + 0.0364 \times DA_{A,NCEP} - 0.00838$ PDO $+ 0.04$	0.66	CAI_{84}: 0.25	0.34
Fram Strait	SON	$V_i = 0.00404 \times CAI_{82} + 0.09$	0.22		0.20

[a]In the right side of each regression equation, the variables are listed in their order of importance, ranked on the basis of the p value. V_i, is in m s^{-1} and CAI is in hPa. Only statistically significant ($p < 0.05$) regression equations are shown. When a multiple regression yields a higher r^2 than a bilateral regression, also the best bilateral r^2 between a circulation index and V_i is given, denoted by BL-r^2. The bilateral r^2 between the air-ice momentum flux and V_i is denoted by τ-r^2 and given when statistically significant.

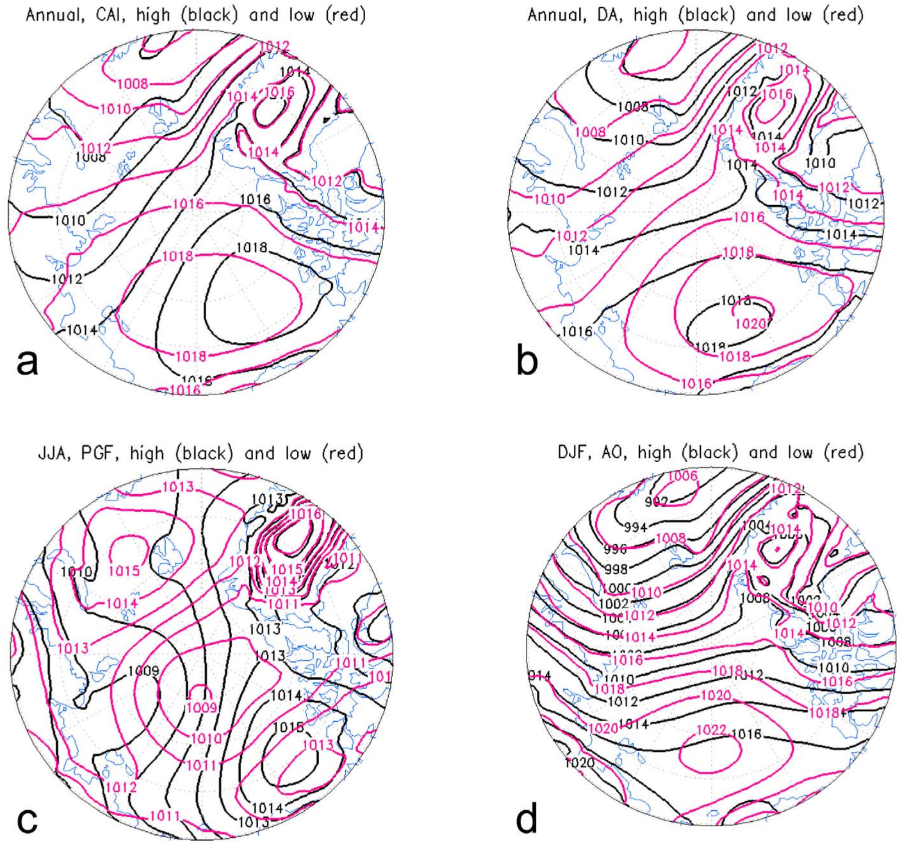

Figure 3. Sea level pressure field (in hPa) averaged over years of four highest (black lines) and four lowest (red lines) values of (a) annual CAI_{82}, (b) $DA_{S,NCEP}$ (c) PGF in JJA, and (d) AO in DJF. The isobars are drawn with 2 hPa intervals, except in Figure 3c.

a SLP pattern strongly favoring transpolar drift and a high V_i (Figure 3c). NAO was nowhere the most important factor to explain V_i. AO appears in only one regression equation in Table 1, but in the Canadian Basin it alone provides the best explanation for V_i in DJF. A low AO allows more advection of ice from the Beaufort Sea westward into the Chuckhi Sea, resulting in a higher V_i, as ice is not so much packed against the Canadian archipelago (Figure 3d).

[14] In addition to the scalar V_i, we analyzed the southward drift component in the Fram Strait. The results revealed significant regression equations in three seasons, with CAI_{80} as the most important factor in spring ($r^2 = 0.53$) and autumn ($r^2 = 0.20$), and $DA_{S,ERA}$ in summer ($r^2 = 0.55$). The southward drift prevailed: only in one spring (2009), autumn (2007), and winter (1999–2000) the seasonal mean ice drift was northwards (note that in the Fram Strait the buoy data only cover area north of 80°N). These seasons were associated with a strong high over the Barents Sea with a northward geostrophic wind, and among the circulation indices the seasons were manifested as highest or second highest absolute values in PDO (spring 2007 and winter 1999–2000) and NAO (autumn 2007 and winter 1999–2000).

[15] V_i showed significant (confidence level $p < 0.05$) increasing trends for the annual mean, JJA, and SON in the Circumpolar Arctic, for annual mean and SON in Eastern Arctic, and for the annual mean, DJF, JJA, and SON in Canadian Basin, but none of the large-scale circulation indices showed trends that could explain the increasing trend in V_i (compare to Figure 2). ERA-Interim V_{10} and τ did have significant positive trends in the Fram Strait, but trends in V_i were not significant there. As regional means in the Eastern Arctic and Canadian basin, all significant trends in V_{10} and τ were negative.

[16] τ was better than V_{10} in statistically explaining interannual variations in V_i but, in general, τ was less good than

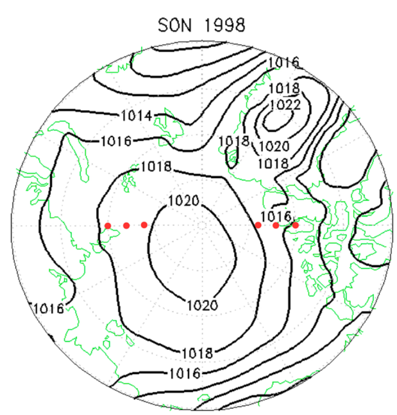

Figure 4. Sea level pressure field (in hPa) in SON 1998 as an example of years with a low CAI and a low ice drift speed but a high DA. The red dots mark the data points used in calculation of CAI_{80}, CAI_{82}, and CAI_{84}.

the large-scale circulation index best for each region and season (Table 1). See Section 4 for our interpretation of this.

4. Discussion

[17] Among the circulation indices studied, CAI was the best in explaining inter-annual variations in V_i. The importance of CAI over the other circulation indices is related to TDS. Although the orientation of TDS varies [*Kwok*, 2009], CAI quantifies the pressure gradient over a fixed line approximately perpendicular to the mean orientation of TDS, whereas the pressure patterns affecting DA sometimes move to locations less essential from the point of view of ice drift (Figures 3 and 4). *Overland and Wang* [2010] pointed out that DA is usually oriented on an Alaska - Kara Sea axis, but in summer more on axis through the Fram Strait. Hence, it is understandable that we observed the strongest relationship between DA and V_i in the Fram Strait in summer. Also the pressure patterns controlling the value of AO have recently varied [*Zhang et al.*, 2008; *Stroeve et al.*, 2011], which may have reduced the effect of AO on V_i.

[18] CAI also has the benefit of being a simple index, which is not sensitive to the calculation method applied (CAI_{80}, CAI_{82}, and CAI_{84} were highly correlated). Instead, in the principal component analysis the second mode is sensitive to the time period of data applied, and therefore DA_S differed a lot from DA_A (Figure 2, $r < 0.2$). Also, $DA_{S,ERA}$ did not equal $DA_{S,NCEP}$ ($r = 0.69$). Further, the second mode is also sensitive to the size of the calculation area [*Overland and Wang*, 2010]. Following *Wu et al.* [2006] and *Wang et al.* [2009], we used 70°N as the southern border of the calculation area, but found out that using 60°N instead, the sensitivity of $DA_{S,M}$ was of the same order of magnitude as the sensitivity to selection between ERAI and NCEP reanalyses. *Hakkinen et al.* [2008] stressed the importance of individual storms on the ice drift. One potential reason for the stronger relationship of V_i with CAI, PGF, and DA compared to AO, NAO, and PDO is that storm effects on the pressure gradient are best taken into account in indices that are based on pressure differences over spatial scales smaller than the typical radius of storms. In indices such as AO, NAO, and PDO, the effects of individual storms are not always detectable.

[19] It is not surprising that V_i is so well explained by CAI. Already *Zubov* [1943] demonstrated the strong effect of the geostrophic wind on the Arctic sea ice drift, and *Thorndike and Colony* [1982] showed that in time scales of days to weeks more than 70% of the ice motion variance was explained by the local geostrophic wind. Compared to the above-mentioned studies, the new aspects in our results are that (1) we analyzed inter-annual variations and (2) instead of comparing the local geostrophic wind to the local V_i, we show that the geostrophic wind components at the North Pole and across the Fram Strait explain a significant part of the variance of the annual and seasonal mean V_i in the Circumpolar and Eastern Arctic, Canadian Basin, and the Fram Strait, although not in all seasons in all regions. The part of the V_i variance not explained by the circulation indices originates from (1) differences between the local, direct atmospheric forcing on ice drift and that represented by the indices, (2) effects of the ocean currents and internal resistance of the ice field, (3) errors in the V_i field (above all the coarse spatial resolution) and in the circulation indices.

[20] *Spreen et al.* [2011] presented thorough comparisons of V_i and V_{10}, but we note that the ERA-Interim V_{10} was in no region and no season as good as τ in explaining variations in V_i. This is because τ provides the direct forcing for V_i, and τ depends not only on V_{10} but also on the surface aerodynamic roughness and, above all, the near-surface stratification [e.g., *Vihma et al.*, 2003]. In general, however, τ was less good than the large-scale circulation indices in explaining inter-annual variations in V_i (Table 1). Only in the Fram Strait does the annual mean V_i correlate better with τ than with the best circulation index (CAI_{82}). In the Fram Strait the ice concentration is on average smaller than in the Central Arctic, which favors free wind-driven drift without much contribution from the internal stress of the ice field. In the Eastern Arctic and especially in the Canadian Basin, the ice is less free to drift according to the local τ, and the strongest statistical relationships were found for such circulation indices (CAI, PGF, DA) whose positive values favor ice drift along the direction where the coastal resistance is smallest, i.e., along the TDS. Another reason reducing the correlations of V_i with τ and V_{10} is the liability of near-surface variables to modeling errors [*Tisler et al.*, 2008].

[21] *Hakkinen et al.* [2008] concluded that the increasing trend in V_i since 1950s, both in summer and winter, is mostly due to increased wind stress, which has resulted from increased storm activity over TDS. Focusing on the shorter period of 1989–2009 we found that neither the large-scale circulation indices nor the near-surface variables (τ and V_{10}) explained the increasing trends in V_i in our three study regions, although over smaller areas in the Central Arctic positive trends in V_i and V_{10} are collocated [*Spreen et al.*, 2011]. Contrary to the trends, a large part of the inter-annual variance in V_i during 1989–2009 is explained by the atmospheric forcing, with CAI as the most relevant circulation index.

[22] **Acknowledgments.** We thank Juhani Rinne, Sirpa Hakkinen, and two anonymous reviewers for valuable comments on the manuscript. The ECMWF, IABP, NOAA, the University of Washington, and Maria Tsukernik at Brown University, Rhode Island, are acknowledged for data supply. This study was supported by the DAMOCLES project, which was funded by the European Commission in the 6th Framework Programme for Research and Development (contract 018509).

[23] The Editor thanks two anonymous reviewers for their assistance in evaluating this paper.

References

Draper, N. R., and H. Smith (1998), *Applied Regression Analysis*, 736 pp., Wiley-Intersci., Hoboken, N. J.

Gascard, J.-C., et al. (2008), Exploring Arctic transpolar drift during dramatic sea ice retreat, *Eos Trans. AGU*, *89*(3), 21, doi:10.1029/2008EO030001.

Hakkinen, S., A. Proshutinsky, and I. Ashik (2008), Sea ice drift in the Arctic since the 1950s, *Geophys. Res. Lett.*, *35*, L19704, doi:10.1029/2008GL034791.

Kwok, R. (2009), Outflow of Arctic sea ice into the Greenland and Barents seas: 1979–2007, *J. Clim.*, *22*, 2438–2457, doi:10.1175/2008JCLI2819.1.

Maslanik, J., S. Drobot, C. Fowler, W. Emery, and R. Barry (2007), On the Arctic climate paradox and the continuing role of atmospheric circulation in affecting sea ice conditions, *Geophys. Res. Lett.*, *34*, L03711, doi:10.1029/2006GL028269.

Ogi, M., I. G. Rigor, M. G. McPhee, and J. M. Wallace (2008), Summer retreat of Arctic sea ice: Role of summer winds, *Geophys. Res. Lett.*, *35*, L24701, doi:10.1029/2008GL035672.

Ogi, M., K. Yamazaki, and J. M. Wallace (2010), Influence of winter and summer surface wind anomalies on summer Arctic sea ice extent, *Geophys. Res. Lett.*, *37*, L07701, doi:10.1029/2009GL042356.

Overland, J. E., and M. Wang (2010), Large-scale atmospheric circulation changes associated with the recent loss of Arctic sea ice, *Tellus, Ser. A*, *62*, 1–9.

Rampal, P., J. Weiss, and D. Marsan (2009), Positive trend in the mean speed and deformation rate of Arctic sea ice, 1979–2007, *J. Geophys. Res.*, *114*, C05013, doi:10.1029/2008JC005066.
Rigor, I. (2002), IABP drifting buoy, pressure, temperature, position, and interpolated ice velocity, http://nsidc.org/data/g00791.html, Polar Sci. Cent., Appl. Phys. Lab., Univ. of Wash., Seattle, Natl. Snow and Ice Data Cent., Boulder, Colo.
Rigor, I. G., and J. M. Wallace (2004), Variations in the age of Arctic seaice and summer sea-ice extent, *Geophys. Res. Lett.*, *31*, L09401, doi:10.1029/2004GL019492.
Spreen, G., R. Kwok, and D. Menemenlis (2011), Trends in Arctic sea ice drift and role of wind forcing: 1992–2009, *Geophys. Res. Lett.*, *38*, L19501, doi:10.1029/2011GL048970.
Stroeve, J. C., M. C. Serreze, I. Rigor, W. Meier, and C. Fowler (2011), Sea ice response to an extreme negative phase of the Arctic Oscillation during winter 2009/2010, *Geophys. Res. Lett.*, *38*, L02502, doi:10.1029/2010GL045662.
Thorndike, A. S., and R. Colony (1982), Sea ice motion in response to geostrophic winds, *J. Geophys. Res.*, *87*, 5845–5852, doi:10.1029/JC087iC08p05845.
Tisler, P., T. Vihma, G. Müller, and B. Brümmer (2008), Modelling of warm-air advection over Arctic sea ice, *Tellus, Ser. A*, *60*, 775–788.
Tsukernik, M., C. Deser, M. Alexander, and R. Thomas (2010), Atmospheric forcing of Fram Strait se ice eport: A closer look, *Clim. Dyn.*, *35*, 1349–1360, doi:10.1007/s00382-009-0647-z.
Vihma, T., and J. Launiainen (1993), Ice drift in the Weddell Sea in 1990–1991 as tracked by a satellite buoy, *J. Geophys. Res.*, *98*, 14,471–14,485, doi:10.1029/93JC00649.
Vihma, T., J. Hartmann, and C. Lüpkes (2003), A case study of an on-ice air flow over the Arctic marginal sea ice zone, *Boundary Layer Meteorol.*, *107*, 189–217, doi:10.1023/A:1021599601948.
Vihma, T., J. Jaagus, E. Jakobson, and T. Palo (2008), Meteorological conditions in the Arctic Ocean in spring and summer 2007 as recorded on the drifting ice station Tara, *Geophys. Res. Lett.*, *35*, L18706, doi:10.1029/2008GL034681.
Wang, J., J. Zhang, E. Watanabe, M. Ikeda, K. Mizobata, J. E. Walsh, X. Bai, and B. Wu (2009), Is the dipole anomaly a major driver to record lows in Arctic summer sea ice extent?, *Geophys. Res. Lett.*, *36*, L05706, doi:10.1029/2008GL036706.
Wu, B., J. Wang, and J. E. Walsh (2006), Dipole anomaly in the winter Arctic atmosphere and its association with sea ice motion, *J. Clim.*, *19*, 210–225, doi:10.1175/JCLI3619.1.
Zhang, X., A. Sorteberg, J. Zhang, R. Gerdes, and J. C. Comiso (2008), Recent radical shifts of atmospheric circulations and rapid changes in Arctic climate system, *Geophys. Res. Lett.*, *35*, L22701, doi:10.1029/2008GL035607.
Zubov, N. N. (1943), *Arctic Ice* (in Russian), 360 pp., Moscow. (English translation, U.S. Naval Oceanogr. Off. and Am. Meteorol. Soc., San Diego, Calif., 491 pp., 1963.

P. Tisler and T. Vihma, Finnish Meteorological Institute, PO Box 503, FI-00101 Helsinki, Finland. (timo.vihma@fmi.fi)
P. Uotila, CSIRO Marine and Atmospheric Research, Aspendale, Vic 3195, Australia.